# Direct Estimation of Acceleration and Jerk of Re-entry Ballistic Targets

**Shrabani Ghosh[a,1], Siddhartha Mukhopadhyay[a]**
[a]Integrated Test Range, Defence Research & Development Organisation, Balasore, Orissa, India
[b]Department of Electrical Engineering, Indian Institute of Technology Kharagpur, West Bengal, India

**Abstract**
An acceleration model and a jerk model are proposed in this paper for kinematic state estimation of re-entry ballistic targets. The models proposed here use fully coupled equations of the target kinematics, without assuming any model structure for variations of ballistic coefficient and air density as found in the literature. The novelty of the algorithms lies in the bootstrapped computation of the model parameter $\gamma$, which is the ratio of air density and ballistic coefficient, at every time step, utilizing the estimated velocity and acceleration. $\gamma$ and its time derivatives, thus computed, are used for parameterization of DA and DJ models for estimating position, velocity and acceleration. This makes the algorithms inherently adaptive to the variations of the ballistic coefficient and the air density during the re-entry trajectory. It is demonstrated that the proposed models produce unbiased estimates of target acceleration as opposed to biased estimates from the existing models.

**Key words:** Ballistic Target Tracking, Extended Kalman Filter, Endo-atmospheric Engagement.

## 1. INTRODUCTION

Accurate estimation of kinematic state of re-entry ballistic targets (RBT) is one of the prime requirements for guidance computation of an interceptor. The Proportional Navigation (PN) guidance utilises the target-interceptor relative kinematics in the form of closing velocity ($V_c$) and sight line rates ($\dot{\lambda}$), whereas the Augmented Proportional Navigation (APN) requires the target accelerations as well for computation of commanded lateral acceleration. Since, these variables are not directly measurable, these are estimated using noisy measurements from ground radars and/or on-board seekers. Given the guidance and control specifications as well as the interceptor capability, the miss distance achieved is determined by the accuracy of estimates of target kinematics.

The estimation accuracy, in turn, is determined by the choice of state and measurement models as well as estimation algorithm and its parameters. The uncertainties in modelling the kinematics of RBTs arise from the unknown mass, the so called reference area, the variation of drag and lift coefficients with Mach number and angle of attack. Coupled to these are the effect of empirical models used for air density and gravity.

Various estimation algorithms reported in the literature for this application include $\alpha-\beta-\gamma$ filter [7, 12,24], Kalman Filter [2,7,12,24], Extended Kalman Filter (EKF) [2,23] and its variants, second order EKF, Extended Interval KF [5], Iterative EKF [1,9], adaptive EKF [3,14,18], unknown Input Estimator [8], Covariance Analysis DEscribing function Technique (CADET) [2,14], Unscented KF (UKF) [14,18,19], Particle Filter (PF) [4,14,18] and its variants namely, Monte Carlo (MC) estimator [13,17], Sampling/Importance Re-sampling (SIR) filter [21], etc., Maximum Likelihood Estimator (MLE) [22], Interacting Multiple Model (IMM) [12,20,22]. Minvielle [24] presents a chronological evolution of these estimation algorithms and their comparative merits and demerits in tracking RBTs. In most of

*Email addresses:* shrabani. g@gmail.com (Shrabani Ghosh), smukh@ee.iitkgp.ernet.in (Siddhartha Mukhopadhyay)
[1]Corresponding author

these estimators, either target acceleration is assumed to be constant [3] or position and velocity are jointly estimated with drag coefficient ($\alpha_d$) or ballistic coefficient ($\beta$) or its function, assuming a particular empirical model for its dynamics. In [1,3,9,13] $\alpha_d$ is modelled as a constant with additive white noise. $\beta$ is assumed to be known in [17, 14]. Further, a constant $\beta$ with additive white noise has been estimated with the kinematic state in [14,18,20,21,22,23]. An empirical model of $\beta$ as a function of altitude has been considered in [5,11]. Li and Jilkov [11] present a survey of these different dynamic model structures for RBTs, in terms of the choice of state and output variables, variations of ballistic coefficients, etc.

However, it can be noted that the ballistic coefficient $\beta$ is constant only for highly supersonic targets [14]. It diminishes when the target velocity approaches Mach 1, due to formation of shock waves. For a typical trajectory, $\beta$ may undergo about 15% variation in endo-atmospheric phase before interception. It can also vary for maneuvering or spiralling targets due to the variation in the angle of attack. Hence, the assumption of constant $\beta$ is not justifiable. First order or random walk models for $\beta$ are also empirical and cannot model the variations adequately. Values of the ballistic coefficient are unknown and vary widely among the RBTs. Hence, the assumption of known $\beta$ is also not tenable. Thus, the accuracy of acceleration computed from the estimated velocity and model parameters $\alpha_d$ or $\beta$ or $\gamma$ is governed by the accuracy of the assumed empirical model.

These limitations of empirical models for parameterization of the state models are alleviated in the present paper. Here two kinematic models of RBTs are proposed which estimate the target acceleration and jerk directly. The significant features of the proposed schemes are summarized below.

- A Direct Acceleration (DA) model is proposed here to estimate position, velocity and acceleration. This model does not assume that the acceleration is a constant plus a random walk noise. Rather, the time derivative of acceleration is modelled in terms of the estimates of kinematic state and that of $\gamma$, $\dot{\gamma}$ as given below. Using a similar approach, the Direct Jerk (DJ) model estimates position, velocity, acceleration and jerk.
- The variables $\gamma = \frac{\rho}{\beta}$ and its time derivatives are computed in bootstrapped[2] mode using the estimated velocity, acceleration and jerk. The computed $y$ and its derivatives are subsequently utilized for the model parameterization in the estimator employing DA and DJ models.
- Thus, the model parameter, i.e., the ballistic coefficient or a function of it is not a state element of the estimator employing DA/DJ model. No empirical model of air density nor of ballistic coefficient is assumed.

Thus, the estimation accuracy of target kinematics is not affected by the selection of model structure and its parameters for ballistic coefficient. The bootstrapped computation of $y$ and use of it in the kinematic equation at each time step caters for the dynamic variation of this parameter along the target trajectory. Moreover, due to variation in the ballistic coefficient, air density and acceleration due to gravity with altitude, the target experiences substantial change in acceleration in re-entry phase. As a result, the adopted jerk model produces better estimates than that of the acceleration model. The estimates from the proposed algorithms have been compared in this paper with the existing models for a realistic target kinematics and a significant improvement is shown in acceleration estimates.

The paper is organised as follows. Section 2 describes the reported and the proposed models for re-entry ballistic target motion and radar measurement model. The scheme for computation of model parameters $\gamma$ and its time derivatives are discussed in Section 3. This is followed by simulation results and discussions in Section 4. All the notations used through out the paper are enlisted in the List of Symbols.

## 2. MODELLING OF TARGET KINEMATICS

In this section the equations of motion of re-entry ballistic target cast as a state space model and the corresponding measurement model employed for its kinematic state estimation are discussed.

### 2.1. Equations of Motion

The main forces acting on a ballistic target during endo-atmospheric phase are aerodynamic forces (drag and lift), gravity and, depending on the coordinate system (i.e., when considered in Earth fixed

[2]In the present context, bootstrapping refers to coupling of the inputs and the outputs of two computation modules through feedback.

frame), Coriolis and centrifugal forces [1,11,16]. The target motion is modelled based on the following assumptions and the model parameters.

- The flight duration of a ballistic target in re-entry phase is short. Hence, the effect of Earth's rotation in the form of Coriolis acceleration is negligible.
- For a flat-Earth assumption, the centrifugal force is negligible.
- The angle of attack for the ballistic re-entry is small. Hence, lift force is neglected. Possible spinning motion at re-entry is also neglected.
- The reference frame for equation of motion is an Earth-fixed VEN (Vertical-East-North) frame.
- Acceleration due to gravity is modelled as

$$g(x) = g_0 \left( \frac{R_e}{R_e + x} \right)^2$$

- The air density for the isothermal layer and the gradient layer of atmosphere is represented by the empirical model given below [5]:

$$\begin{aligned} \rho(x) &= \rho_0 e^{\frac{-g(x-x_0)}{g_c T_1}} \\ &\quad \text{for isothermal layer} \\ &= \rho_0 \left( \frac{T_1 + L_R (x - x_0)}{T_1} \right)^{-(\frac{g}{L_R g_c}+1)} \\ &\quad \text{for gradient layer} \end{aligned} \tag{1}$$

Thus, drag and gravity are the main forces acting on the target in the re-entry phase. The acceleration due to drag is proportional to the dynamic pressure and acts in the direction opposite to the total velocity of the target relative to the atmosphere. Thus, considering the drag and gravity forces, the kinematic equation of motion can be represented as given in (2):

$$\begin{bmatrix} \ddot{x} \\ \ddot{y} \\ \ddot{z} \end{bmatrix} = \begin{bmatrix} \frac{-0.5\rho(x)\dot{x}V}{\beta} - g(x) \\ \frac{-0.5\rho(x)\dot{y}V}{\beta} \\ \frac{-0.5\rho(x)\dot{z}V}{\beta} \end{bmatrix} \tag{2}$$

## 2.2. State Models

Several state models have been reported in the literature. These, as well as the proposed direct acceleration and direct jerk models with bootstrapped estimate of $\gamma$ are discussed below.

### *2.2.1. Existing Models ([1,3,5,8,9,11,13,17,18,20,22,23])*

These models incorporate the dynamics of $\beta$ or its function along with the position and velocity to form the state vector of the target. The state equation for these models can be represented in the generic form as given in (3). Here, the state variable p and its dynamics represented by $h_p$(p) depend on the selection of the model parameter (i.e., ballistic coefficient or its function) and its model structure. The particular choice for these are given below.

$$\frac{d}{dt} \begin{bmatrix} x \\ y \\ z \\ \dot{x} \\ \dot{y} \\ \dot{z} \\ p \end{bmatrix} = \begin{bmatrix} \dot{x} \\ \dot{y} \\ \dot{z} \\ -0.5p\dot{x}V - g(x) \\ -0.5p\dot{y}V \\ -0.5p\dot{z}V \\ h_p(p) \end{bmatrix} + \begin{bmatrix} 0 \\ 0 \\ 0 \\ \omega_{\ddot{x}} \\ \omega_{\ddot{y}} \\ \omega_{\ddot{z}} \\ 0 \end{bmatrix} \tag{3}$$

*Constant Ballistic Coefficient (CBC) ([18,20,21,22,23]).* In this case, $p_{CBC} = \beta$ and the ballistic coefficient is modelled as constant with additive white Gaussian noise as given in (4).

$$\begin{aligned}\dot{\beta} &= h_{\beta}(\beta)\\ &= 0+\omega_{\dot{\beta}}\end{aligned} \tag{4}$$

*Constant Inverse Ballistic Coefficient (CIBC) ([1,9,13,23]).* In this case, $p_{CIBC} = \alpha_d$ and the drag parameter $\alpha_d$ is modelled as constant with additive white Gaussian noise as given in (5).

$$\begin{aligned}\dot{\alpha}_d &= h_{\alpha d}(\alpha d)\\ &= 0+\omega_{\dot{\alpha}_d}\end{aligned} \tag{5}$$

*Composite model of Air Density and Ballistic Coefficient (ADBC) ([5,11]).* In both the previous models given in equations (4) and (5), the air density has been modelled explicitly by using the empirical relation (1). In the case of ADBC, the dynamics of air density and ballistic coefficient are modelled together by defining a new parameter $\gamma = \rho/\beta$, which is augmented with the kinematic state elements for estimation. In this case, an exponential model for air density and a linear variation of $\beta$ with altitude have been assumed as given below in (6) and (7).

$$\rho = \rho_0 e^{-kx} \tag{6}$$

$$\beta = p_0 + p_1 x \tag{7}$$

Combining equations (6) and (7), the following dynamic equation is obtained.

$$\begin{aligned}\dot{\gamma} &= h_{\gamma}(\gamma)\\ &= -C\gamma\dot{x}+\omega_{\dot{\gamma}}\end{aligned} \tag{8}$$

Here, $C = k + \frac{p_1}{p_0+p_1 x}$, $p_0$ and $p_1$ are the design parame-ters whose values are assumed heuristically depending on the type of the target. The selection of air-density parameters $p_0$ and $k$ are also based on empirical models.

### 2.2.2. Proposed Models

Two models for RBTs are proposed here, which compute the target kinematics directly. These models do not include the parameters $\beta$ or $\gamma$ as state elements as in the cases of CBC, CIBC and ADBC. No empirical model for these variables and air density is assumed in these cases. The proposed Direct Acceleration (DA) and Direct Jerk (DJ) models are described below.

*Direct Acceleration Model (DA).* In this case, target position, velocity and acceleration components are directly estimated [10] using the nonlinear state model in (9). It can be noted that, this model does not assume that the acceleration is a constant plus a random noise, as in [3]. However, the time derivative of acceleration is modelled in terms of the kinematic state and that of $\gamma$, $\dot{\gamma}$.

$$\frac{d}{dt}\begin{bmatrix} x\\ y\\ z\\ \dot{x}\\ \dot{y}\\ \dot{z}\\ \ddot{x}\\ \ddot{y}\\ \ddot{z}\end{bmatrix} = \begin{bmatrix} \dot{x}\\ \dot{y}\\ \dot{z}\\ \ddot{x}\\ \ddot{y}\\ \ddot{z}\\ f_{\ddot{x}}\\ f_{\ddot{y}}\\ f_{\ddot{z}}\end{bmatrix} + \begin{bmatrix} 0\\ 0\\ 0\\ \omega_{\ddot{x}}\\ \omega_{\ddot{y}}\\ \omega_{\ddot{z}}\\ \omega_{\dddot{x}}\\ \omega_{\dddot{y}}\\ \omega_{\dddot{z}}\end{bmatrix} \tag{9}$$

Here,

$$\begin{aligned} f_{\ddot{x}} &= -0.5\dot{\gamma}_c\dot{x}V - 0.5\gamma_c\ddot{x}V\\ &\quad - 0.5\gamma_c\dot{x}\dot{V} - \dot{g}(x)\end{aligned} \tag{10}$$

$$f_{\ddot{y}} = -0.5\dot{\gamma}_c \dot{y}V - 0.5\gamma_c \ddot{y}V \\ -0.5\gamma_c \dot{y}\dot{V} \tag{11}$$

$$f_{\ddot{z}} = -0.5\dot{\gamma}_c \dot{z}V - 0.5\gamma_c \ddot{z}V \\ -0.5\gamma_c \dot{z}\dot{V} \tag{12}$$

$$\dot{g}(x) = \frac{-2g_0 R_e^2 \dot{x}}{(R_e + x)^3} \tag{13}$$

$$\dot{V} = \frac{\dot{x}\ddot{x} + \dot{y}\ddot{y} + \dot{z}\ddot{z}}{V} \tag{14}$$

Here, the composite variable $\gamma_c = \rho/\beta$ is computed in bootstrapped mode from the estimated kinematics at every time step for use in the next update cycle as given in Section 3.

*Direct Jerk Model (DJ)*. In this model, the jerk components are also estimated in addition to position, velocity and acceleration [6,10] using the state model given in equation (15). Here also the composite variable $\gamma$ and its first and second derivatives are updated using the estimated kinematics at each time step as described in Section 3. In contrary to constant jerk assumption, the jerk is modelled here in terms of the kinematic state and the parameters $\gamma\ \dot{\gamma}$ , and $\ddot{\gamma}$ as seen in (16)–(18).

$$\frac{d}{dt}\begin{bmatrix} x \\ y \\ z \\ \dot{x} \\ \dot{y} \\ \dot{z} \\ \ddot{x} \\ \ddot{y} \\ \ddot{z} \\ \dddot{x} \\ \dddot{y} \\ \dddot{z} \end{bmatrix} = \begin{bmatrix} \dot{x} \\ \dot{y} \\ \dot{z} \\ \ddot{x} \\ \ddot{y} \\ \ddot{z} \\ \dddot{x} \\ \dddot{y} \\ \dddot{z} \\ f_{\dddot{x}} \\ f_{\dddot{y}} \\ f_{\dddot{z}} \end{bmatrix} + \begin{bmatrix} 0 \\ 0 \\ 0 \\ \omega_{\dot{x}} \\ \omega_{\dot{y}} \\ \omega_{\dot{z}} \\ \omega_{\ddot{x}} \\ \omega_{\ddot{y}} \\ \omega_{\ddot{z}} \\ \omega_{\dddot{x}} \\ \omega_{\dddot{y}} \\ \omega_{\dddot{z}} \end{bmatrix} \tag{15}$$

Here,

$$f_{\dddot{x}} = -0.5\ddot{\gamma}_c \dot{x}V - \dot{\gamma}_c \ddot{x}V - \dot{\gamma}_c \dot{x}\dot{V} - 0.5\gamma_c \dddot{x}V \\ -\gamma_c \ddot{x}\dot{V} - 0.5\gamma_c \dot{x}\ddot{V} - \ddot{g}(x) \tag{16}$$

$$f_{\dddot{y}} = -0.5\ddot{\gamma}_c \dot{y}V - \dot{\gamma}_c \ddot{y}V - \dot{\gamma}_c \dot{y}\dot{V} - 0.5\gamma_c \dddot{y}V \\ -\gamma_c \ddot{y}\dot{V} - 0.5\gamma_c \dot{y}\ddot{V} \tag{17}$$

$$f_{\dddot{z}} = -0.5\ddot{\gamma}_c \dot{z}V - \dot{\gamma}_c \ddot{z}V - \dot{\gamma}_c \dot{z}\dot{V} - 0.5\gamma_c \dddot{z}V \\ -\gamma_c \ddot{z}\dot{V} - 0.5\gamma_c \dot{z}\ddot{V} \tag{18}$$

$$\ddot{g}(x) = \frac{-2g_0 R_e^2 \ddot{x}}{(R_e + x)^3} + \frac{6g_0 R_e^2 \dot{x}^2}{(R_e + x)^4} \tag{19}$$

$$\ddot{V} = \frac{\ddot{x}^2 + \dot{x}\dddot{x} + \ddot{y}^2 + \dot{y}\dddot{y} + \ddot{z}^2 + \dot{z}\dddot{z}}{V} \\ - \frac{(\dot{x}\ddot{x} + \dot{y}\ddot{y} + \dot{z}\ddot{z})^2}{V^3} \tag{20}$$

### 2.3. Measurement Models

For the present study, radar measurements of position and velocity in cartesian frame are considered. Followings are the assumptions for the measurement process.

- The measurements in cartesian frame are obtained by deterministic conversion from spherical measurements.
- Non-zero mean and correlated measurement noise resulting from this nonlinear conversion of measurements is neglected in the present study for simplicity.
- Measurement noise is additive, zero-mean, white and independent in the different measurement components.

The measurement equation in cartesian frame is given by (21).

$$\begin{bmatrix} x_m(t) \\ y_m(t) \\ z_m(t) \\ \dot{x}_m(t) \\ \dot{y}_m(t) \\ \dot{z}_m(t) \end{bmatrix} = HX(t) + \begin{bmatrix} \eta_x(t) \\ \eta_y(t) \\ \eta_z(t) \\ \eta_{\dot{x}}(t) \\ \eta_{\dot{y}}(t) \\ \eta_{\dot{z}}(t) \end{bmatrix} \tag{21}$$

For the different state models considered, the measurement matrix $H$ takes the form as given below:

$$\begin{aligned} H_{CBC} &= H_{CIBC} = H_{ADBC} \\ &= \begin{bmatrix} I_{6\times6} & \vdots & O_{6\times1} \end{bmatrix} \end{aligned} \tag{22}$$

$$H_{DA} = \begin{bmatrix} I_{6\times6} & \vdots & O_{6\times3} \end{bmatrix} \tag{23}$$

$$H_{DJ} = \begin{bmatrix} I_{6\times6} & \vdots & O_{6\times6} \end{bmatrix} \tag{24}$$

## 3. BOOTSTRAPPED COMPUTATION OF $\gamma_c$

The DA and DJ models as given in Equations (9) and (15), use γ and its derivative(s) for their model parameterization. Instead of using an empirical model with pre-decided parameters as in CBC, CIBC and ADBC models, these variables are computed using the estimated kinematic state. Since, the acceleration due to drag is given by $D = \frac{0.5\rho V^2}{\beta}$, $\gamma$ can be computed as

$$\begin{aligned} \gamma_c &= \frac{D}{0.5V^2} \\ &= \frac{\sqrt{(\ddot{x} + g(x))^2 + \ddot{y}^2 + \ddot{z}^2}}{0.5(\dot{x}^2 + \dot{y}^2 + \dot{z}^2)} \end{aligned} \tag{25}$$

The first and second time derivatives of $\gamma_c$ as used in the direct acceleration model and the direct jerk model are given as

$$\dot{\gamma}_c = \frac{2\dot{D}}{V^2} - \frac{4D\dot{V}}{V^3} \tag{26}$$

$$\ddot{\gamma}_c = \frac{2\ddot{D}}{V^2} - \frac{8\dot{D}\dot{V}}{V^3} - \frac{4D\ddot{V}}{V^3} + \frac{12D\dot{V}^2}{V^4} \tag{27}$$

Here,

$$\dot{D} = \frac{(\ddot{x} + g(x))(\dddot{x} + \dot{g}(x)) + \ddot{y}\,\dddot{y} + \ddot{z}\,\dddot{z}}{D} \tag{28}$$

$$\begin{aligned}\ddot{D} = {} & \frac{\left(\dddot{x} + \dot{g}(x)\right)^2 + \left(\ddot{x} + g(x)\right)\left(\ddddot{x} + \ddot{g}(x)\right)}{D} \\ & + \frac{\dddot{y}^2 + \ddot{y}\,\ddddot{y} + \dddot{z}^2 + \ddot{z}\,\ddddot{z}}{D} \\ & - \frac{\left(\left(\ddot{x} + g(x)\right)\left(\dddot{x} + \dot{g}(x)\right) + \ddot{y}\dddot{y} + \ddot{z}\dddot{z}\right)^2}{D^3}\end{aligned} \tag{29}$$

Thus, using the estimated kinematics, $\gamma_c$, $\dot{\gamma}_c$ and $\ddot{\gamma}_c$ can be computed at each time step for use in the next update cycle in the direct acceleration and the direct jerk models.

## 3.1. Computation of $\gamma_c$, $\dot{\gamma}_c$ and $\ddot{\gamma}_c$ for DA Model

Since, jerk used in (28) for computation of $\dot{\gamma}_c$, is not a state variable in the DA model, an iterative computation of it from (9) at each time step is needed and is given below.

- Step 1: Neglecting the jerk terms in (28), $\dot{\gamma}_c$ is calculated using the equation (30) below and (14) based on the estimated position, velocity and accelerations.

$$\dot{\gamma}_c = \frac{2\dot{g}(\hat{x})(\hat{\ddot{x}} + g(\hat{x}))}{\hat{D}\hat{V}^2} - \frac{4\hat{D}\dot{\hat{V}}}{\hat{V}^3} \tag{30}$$

- Step 2: $\dot{\gamma}_c$ is computed using (25).
- Step 3: $\gamma_c$, and $\dot{\gamma}_c$ thus computed are used in equations (10)-(12) to compute jerk components from (9).
- Step 4: Computed jerk components are now used in (28) for updating $\dot{\gamma}_c$ using (26) for the same time step.

## 3.2. Computation of $\gamma_c$, $\dot{\gamma}_c$ and $\ddot{\gamma}_c$ for DJ Model

As in the previous case, the rate of jerk and $\ddot{\gamma}_c$ are computed as stated below.

- Step 1: Neglecting the rate of jerks in (29), $\ddot{\gamma}_c$ is calculated using the equation (31) below and (20) based on estimated position, velocity, acceleration and jerk.

$$\begin{aligned}\ddot{\gamma}_c = {} & \frac{2\Big(\big(\hat{\dddot{x}} + \dot{g}(\hat{x})\big)^2 + \ddot{g}(\hat{x})\Big(\hat{\ddot{x}} + g(\hat{x})\Big) + \hat{\dddot{y}}^2 + \hat{\dddot{z}}^2\Big)}{\hat{D}\hat{V}^2} \\ & - \frac{2\Big(\Big(\hat{\ddot{x}} + g(\hat{x})\Big)\big(\hat{\dddot{x}} + \dot{g}(\hat{x})\big) + \hat{\ddot{y}}\hat{\dddot{y}} + \hat{\ddot{z}}\hat{\dddot{z}}\Big)^2}{\hat{D}^3\hat{V}^2} \\ & - \frac{8\dot{\hat{D}}\dot{\hat{V}}}{\hat{V}^3} - \frac{4\dot{\hat{D}}\ddot{\hat{V}}}{\hat{V}^3} + \frac{12\hat{D}\dot{\hat{V}}^2}{\hat{V}^4}\end{aligned} \tag{31}$$

- Step 2: $\gamma_c$, and $\dot{\gamma}_c$ are computed using (25) and (26) respectively.
- Step 3: $\gamma_c$, $\dot{\gamma}_c$ and $\ddot{\gamma}_c$ thus computed are used in equations (16)–(18) to compute rate of jerk components from (15).
- Step 4: Computed rates of jerk are used in (29) for updating $\ddot{\gamma}_c$ using (27) for the same time step.

## 4. SIMULATION RESULTS

This section presents the details of the numerical implementation, the criteria chosen for comparative performance assessment, the cases for which the results are presented and finally the numerical results themselves, alongwith a discussion on the results.

### 4.1. Performance Comparison Criteria

- The performance of the two proposed models and the three existing ones are demonstrated by employing five separate Extended Kalman filters (EKF) for a typical re-entry target simulated with the realistic aerodynamic characteristic for a typical class of target. However, this knowledge is not used for design of the estimators.
- Performance has been compared in terms of the mean of estimation error in position, velocity and acceleration and the estimates of acceleration components averaged over 50 Monte Carlo (MC) runs.
- For comparison, the acceleration components for the three existing models are computed from their own estimates of position, velocity and $\beta$, $\alpha_d$ or $\gamma$ as in (32), as in these cases the acceleration components are not available as state elements. However, for the proposed models, the acceleration components are directly used from the estimators.

$$\begin{aligned}\hat{\ddot{x}}(k \mid k) &= -0.5\hat{p}(k \mid k)\hat{\dot{x}}(k \mid k)\hat{V}(k \mid k) - g\left(\hat{x}(k \mid k)\right)\\ \hat{\ddot{y}}(k \mid k) &= -0.5\hat{p}(k \mid k)\hat{\dot{y}}(k \mid k)\hat{V}(k \mid k)\\ \hat{\ddot{z}}(k \mid k) &= -0.5\hat{p}(k \mid k)\hat{\dot{z}}(k \mid k)\hat{V}(k \mid k)\end{aligned} \tag{32}$$

Here, $\hat{p}(k|k)$ for different existing models are computed as given in Table 1.

**Table 1. Computation of $\hat{p}(k|k)$ for the existing models**

| Model | $\hat{\rho}(k\|k)$ |
|---|---|
| CBC | $\frac{\rho(\hat{x}(k\|k))}{\beta(k\|k)}$ |
| CIBC | $\rho(\hat{x}(k\|k))\ \hat{\alpha}_d\ (k\|k)$ |
| ADBC | $\hat{\gamma}(k\|k)$ |

### 4.2. Simulation Conditions

The initial conditions for the target kinematics, measurement noise characteristics, selection of model parameters, initialization of EKF are enunciated below.

- The true target trajectory is simulated with the known mass, reference area and variation of drag coefficient with Mach and angle of attack of a typical target. However, this information is not used in implementation of EKF. The initial trajectory conditions are (34, 9, 13)km in position, (–1, 0.1, –0.2)km/s in velocity and (–5, 0.05, –0.02)m/s$^2$ in acceleration in VEN coordinate system.
- The values of the air density model parameters used in generating the target trajectory are given in Table 2. The same parameters are used in implementation of EKF employing CBC and CIBC models. However, DA and DJ models do not use any such empirical model for air density.

**Table 2. Parameters for Air Density Model**

| Altitude $x_0$ (km) | Temperature $T_1$ (Kelvin) | Lapse Rate $L_R$ (Kelvin/meter) | Layer |
|---|---|---|---|
| 0 | 288.16 | $-6.5 \times 10^{-3}$ | Gradient |
| 11 | 216.66 | 0 | Isothermal |
| 25 | 216.66 | $3.0 \times 10^{-3}$ | Gradient |
| 47 | 282.66 | 0 | Isothermal |

- Measurement data is generated from true position and velocity with additive zero-mean, white noise with the standard deviations (10,10,10)m in position and (0.1,0.1,0.1)m/s in velocity.
- The model parameters in ADBC are assumed as $p_0 = 1.395 \times 10^5$ kg/m$^2$, $p_1 = -1.248$ kg/m$^3$ for the trajectory considered. Further, $k = 1.491 \times 10^{-4}$ m$^{-1}$ and $\rho_0 = 1.752$ kg/m$^3$ for altitude $\geq 9.1$ km.
- The estimators are initialized with the first sample of measurements for CBC, CIBC and ADBC. In these cases, $\beta$ is initialised as 35000 kg/m$^2$.
- For DA and DJ models, first two samples of measurements are used for initialization of the position, velocity and acceleration state. The jerk elements are initialized as zero in the DJ model.
- The model noise variance for each of the models has been tuned to attain best performance for the corresponding model.
- Fifty Monte Carlo runs for each of the models have been executed by varying the measurement noise sequence.

### 4.3. Simulation Results and Discussions

The performances of EKFs using the different kinematic models averaged over 50 MC runs are shown in Fig. 1-9 in terms of estimation errors in position and velocity along x, y and z directions as well as acceleration estimates.

It is clear that EKF for all the models yields zero-mean estimation error in position and velocity. Further, the mean and variance of the estimation errors in position and velocity for all the models are comparable. This is because of the use of position and velocity measurements for state update. The significance of the proposed DA and DJ algorithms are apparent in the case of acceleration estimates. It is clear from Figs. 7-9 that the DA and DJ models produce acceleration estimates with zero mean error, whereas the estimates from CBC, CIBC and ADBC models are biased. This is because the assumption of contsant $\beta$ in CBC and CIBC models and the selection of models parameters $p_0$, $p_1$ in ADBC do not conform to the actual variation of $\beta$ in the true target trajectory. However, the proposed DA and DJ models use $\gamma$ and its derivatives computed from the estimated position and velocity, without presuming any empirical model structure and thus are capable of capturing the variation in these model parameters adequately. As a consequence, the acceleration estimates closely follow the true target acceleration with zero mean estimation error. However, the variance of acceleration estimates are higher in case of DA and DJ as opposed to the existing models. This is due to bootstrapped estimation of model parameters.

It is to be noted that, significant bias present in acceleration estimates from CBC, CIBC and ADBC models are more detrimental for guidance application, than presence of zero mean estimation error with higher variance. Large bias in the estimates of velocity and acceleration may result in high demand of lateral acceleration, which may lead to saturation of the actuators. However, the actuator bandwidth limits the high frequency noise in the acceleration estimates resulted from the higher variance. Thus, the acceleration estimates employing the proposed DA and DJ models are promising for use in guidance application because of its unbiased estimates, inspite of yielding higher variance in acceleration estimates.

## 5. CONCLUSION

In this paper, two novel algorithms have been proposed which estimates the acceleration and the jerk of the reentry ballistic targets employing bootstrapped computation of model parameters $\gamma$, $\dot{\gamma}$ and $\ddot{\gamma}$. It has been demonstrated that the proposed direct acceleration model and direct jerk model produce unbiased estimates of acceleration in contrary to the biased estimates from the existing models. The proposed models can adequately represent the variation in $\rho$ and $\beta$ through the bootstrapped computation of $\gamma = \frac{\rho}{\beta}$ using the estimated kinematics. Although the incorporation of acceleration and jerk as the state elements in the proposed models increases the computational requirement, however, the advantage obtained through accurate and unbiased estimates of acceleration makes these algorithms promising for employing in closed loop interceptor guidance.

## 6. REFERENCES

[1] R K Mehra, ‘A Comparison for Several Nonlinear Filters for Reentry Vehicle Tracking’, *IEEE Transactions on Automatic Control,* Vol. AC-16, No. 4, 1971.

[2] A Gelb, ‘Applied Optimal Estimation’, Cambridge MA, MIT Press, 1974, pp. 216-224.

[3] C B Chang, R H Whiting, M Athans, ‘On the State and Parameter Estimation for Maneuvering Reentry Vehicles’, *IEEE Transaction on Automatic Control,* February, 1977, pp. 99-105.

[4] N J Gordon, D J Salmond, A F M Smith, ‘Novel approach to nonlinear/non-Gaussian Bayesian state estimation’, *IEE Proceedings,* Vol. 140, NO. 2, April 1993, pp. 107-113.

[5] G M Siouris, J Wang, ‘Tracking an Incoming Ballistic Missile Using an Extended Interval Kalman Filter ’, IEEE Transaction on Aerospace and Electronic Systems, Vol. 33, No. 1, January 1997, pp. 232-240.

[6] K Mehrotra, P R Mahapatra, ‘A Jerk Model for Tracking Highly Maneuvering Targets’, IEEE Transaction on Aerospace and Electronic Systems, Vol. 33, No. 4, October 1997, pp. 1094-1105.

[7] J A Lawton, R J Jesionowski, P Zarchan, ‘Comparison of Four Filtering Options for a Radar Tracking Problem’, Journal of Guidance, Control and Dynamics, Vol. 21, No. 4, July-August 1998, pp. 618-624.

[8] S C Lee, Y C Huang, C Y Liu, ‘Trajectory Estimation for Tactical Ballistic Missiles in Terminal Phase Using On-line Input Estimator’, *Proceedings of National Science Council ROC(A),* Vol. 23, No. 5, 1999, pp. 644-653.

[9] G P Cardillo, A V Mrstik, T Plambeck, ‘A Track filter for Reentry Objects with Uncertain Drag’, *IEEE Transaction on Aerospace and Electronic Systems,* Vol. 35, No. 2, April, 1999, pp. 394-409.

[10] P R Mahapatra, K Mehrotra, ‘Mixed Coordinate Tracking of Generalized Maneuvering Targets Using Acceleration and Jerk Models’, IEEE Transaction on Aerospace and Electronic Systems, Vol. 36, No. 3, July 2000, pp. 992-1000.

[11] X. Rong Li and Vesselin P. Jilkov, ‘A Survey of Maneuvering Target Tracking-Part II: Ballitic Target Models’, *Proceedings of SPIE Conference on Data and Signal Processing of Small Targets,* San Diego, CA, USA, July-August 2001.

[12] Y Bar-Shalom, X Rong Li, T Kirubarajan, ‘Estimation with Applications to Tracking and Navigation’, Wiley Interscience Publication, John Wiley & Sons Inc., USA, 2001.

[13] P Minvielle, ‘Tracking a Ballistic Re-entry Vehicle with a Sequential Monte-Carlo Filter’, *Proceedings of IEEE Aerospace Conference,* 2002, pp. 4-1773-4-1787.

[14] A Farina, B Ristic, D Benvenuti, ‘Tracking a Ballistic Target: Comparison of Several Nonlinear Filters’, *IEEE Transactions on Aerospace and Electronic Systems,* Vol. 38, No. 3, July 2002.

[15] P Zarchan, ‘Tactical and Strategic Mssile Guidance’, Forth edition, American Institute of Aeronautics and Astronautics Inc., Virginia, 2002.

[16] Brian L Stevens, Frank L Lewis, ‘Aircraft Control and Simulation’, Second Edition, John Wiley and Sons Inc., New Jersey, 2003.

[17] D Angelova, I Simeonova, T Semerdjiev, ‘Monte Carlo Algorithm for Ballistic Object Tracking with Uncertain Drag Paramater’, *Large Scale Scientific Computing 2003,* Bulgaria, pp. 112-120.

[18] B Ristic, A Farina, D Benvenuti, M S Arulampalam, ‘Perofrmance bounds and Comparison of Nonlinear Filters for Tracking a Ballistic Object on Re-entry’, *IEE Proceedings on Radar Sonar and Navigation,* Vol. 150, No. 2, April 2003, pp. 65-70.

[19] S J Julier, J K Uhlmann, ‘Unscented filtering and nonlinear estimation’, *Proceedings of the IEEE,* Vol. 92, No. 3, March 2004, pp. 401-422.

[20] A Farina, M G Del Gaudio, U D Elia, S Immediata, L Ortenzi, L Timmoneri, M R Toma, ‘Detection and Tracking of Ballistic Target’, *Proceedings of IEEE Radar Conference,* 2004, pp. 450-456.

[21] M G S Bruno, A Pavlov, ‘Improved Sequential Monte Carlo Filtering for Ballistic Target Tracking’, *IEEE Transactions on Aerospace and Electronic Systems,* Vol. 41, No. 3, July 2005.

[22] A. Farina, ‘Comparison of Recursive and Batch Processing for Impact Point Prediction of Ballistic Targets’, *IEEE International Radar Conference,* 2005, pp. 121-126.

[23] P N Divedi, A Bhattacharya,P Bhale, ‘Fast Convergence of Ballistic Coefficient to Estimate Re-entry Vehicle Acceleration using EKF from Noisy RF Seeker Data’, *Proceedings of National Systems Conference,* India, 2005.

[24] P Mnvielle, ‘Decades of Improvements in Re-entry Ballistic Vehicle Tracking’, *IEEE Aerospace and Electronic Systems Magazine,* August 2005.

## LIST OF SYMBOLS

| | |
|---|---|
| $C_d$ | Drag coefficient |
| $C_l$ | Lift coefficient |
| $A_s$ | Reference cross-sectional area |
| $m$ | Mass |
| $\alpha_d$ | Drag parameter $= \frac{C_d A_s}{m}$ |
| $\beta$ | Ballistic coefficient $= \frac{1}{\alpha_d}$ |
| $\dot{\beta}$ | Time derivative of $\beta$ |
| $\rho(x)$ | Air density at altitude $x$ |
| $L_R$ | Lapse rate |
| $g_c$ | Gas constant (J/kg-K) |
| $T_1$ | Temperature (K) at bottom of each layer |
| $x_0$ | Lower bound for altitude of each layer |
| $\rho_0$ | Air density corresponding to altitude $x_0$ for each layer |
| $g(x)$ | Acceleration due to gravity |
| $g_0$ | Acceleration due to gravity on the surface of the Earth |
| $R_e$ | Radius of Earth |
| $x, y, z$ | Target position components |
| $\dot{x}, \dot{y}, \dot{z}$ | Target velocity components |
| $\ddot{x}, \ddot{y}, \ddot{z}$ | Target acceleration components |
| $\dddot{x}, \dddot{y}, \dddot{z}$ | Target jerk components |
| $\ddddot{x}, \ddddot{y}, \ddddot{z}$ | Rate of jerk components |
| $V$ | Total taregt velocity |
| $D$ | Acceleration due to drag |
| $\omega_{\ddot{x}}, \omega_{\ddot{y}}, \omega_{\ddot{z}}$ | Zero-mean and white process noise components of accelerations |
| $\omega_{\dddot{x}}, \omega_{\dddot{y}}, \omega_{\dddot{z}}$ | Zero-mean and white process noise components of jerks |
| $\omega_{\ddddot{x}}, \omega_{\ddddot{y}}, \omega_{\ddddot{z}}$ | Zero-mean and white process noise components of rate of jerks |
| $\omega_{\dot{\beta}}$ | Zero-mean and white process noise for $\dot{\beta}$ |
| $\omega_{\dot{\alpha}_d}$ | Zero-mean and white process noise for $\dot{\alpha}_d$ |
| $\omega_{\dot{\gamma}}$ | Zero-mean and white process noise for $\dot{\gamma}$ |
| $\eta_x, \eta_y, \eta_z$ | Measurement noise in position components |
| $\eta_{\dot{x}}, \eta_{\dot{y}}, \eta_{\dot{z}}$ | Measurement noise in velocity components |
| $X(k)$ | State vector at $k$-th instant |
| $X(k\|k)$ | Estimated state vector at $k$-th instant |
| $P(k\|k)$ | State estimation error covariance |
| $I_{n\times n}$ | $n \times n$ Identity matrix |
| $O_{n\times m}$ | $n \times m$ Zero matrix |

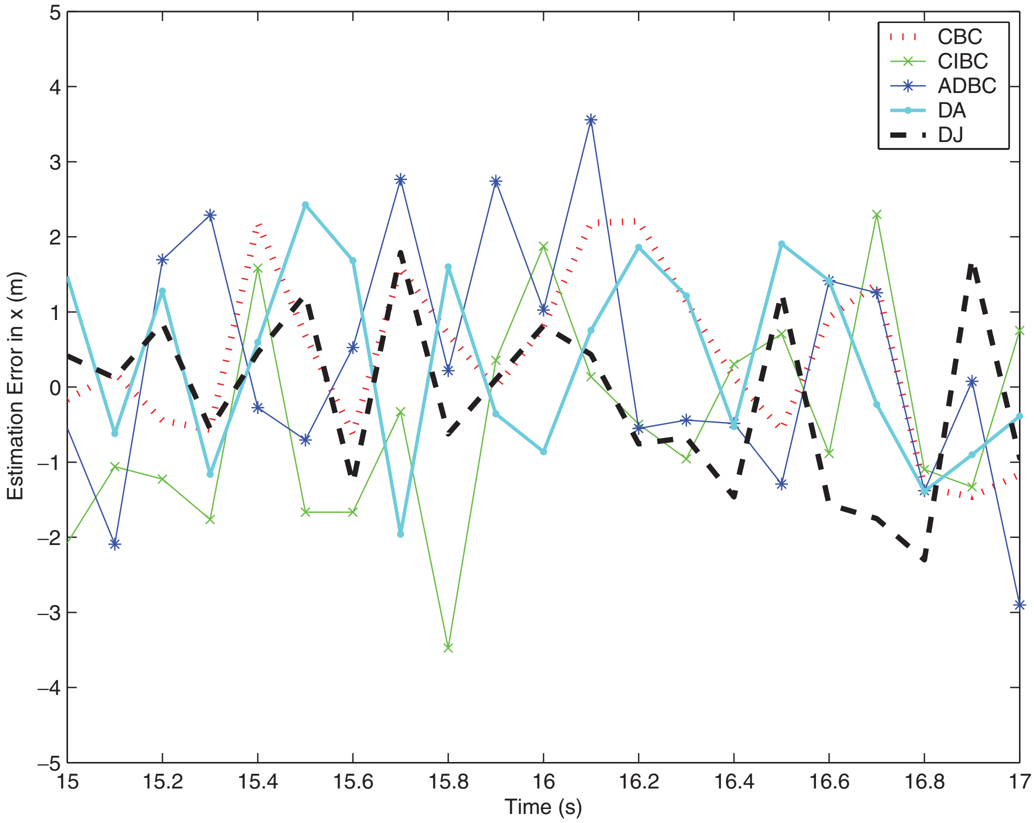


Figure 1. Position estimation error in X

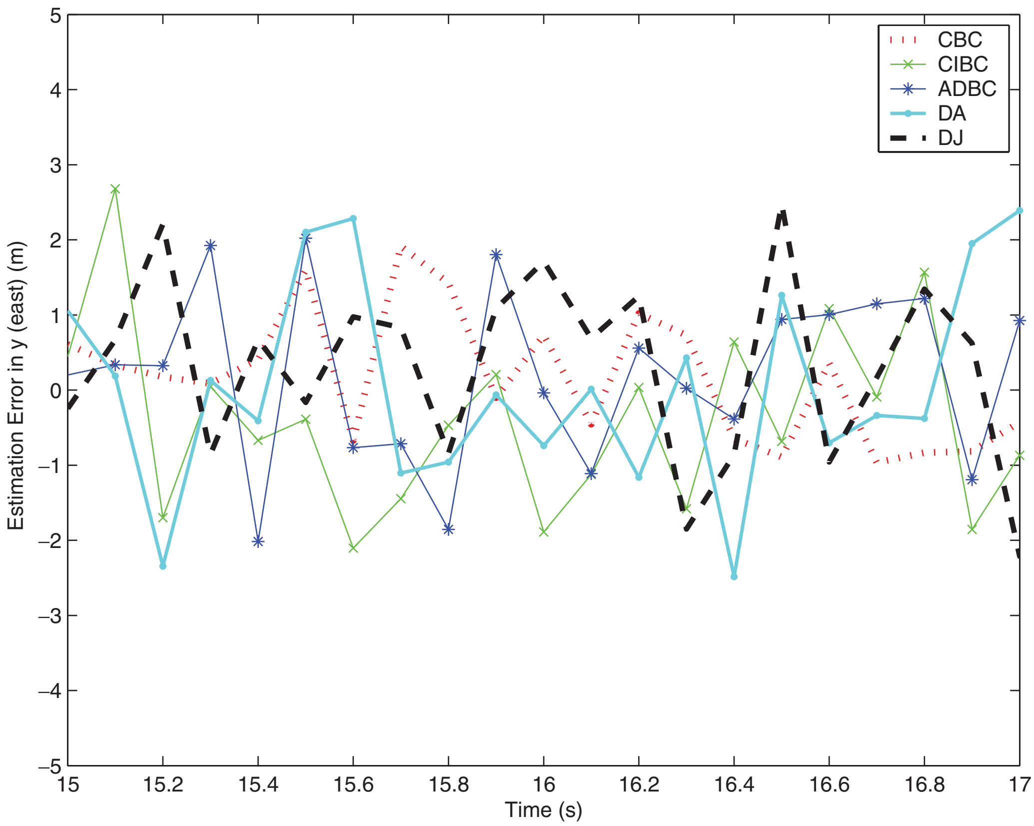


Figure 2. Position estimation error in Y

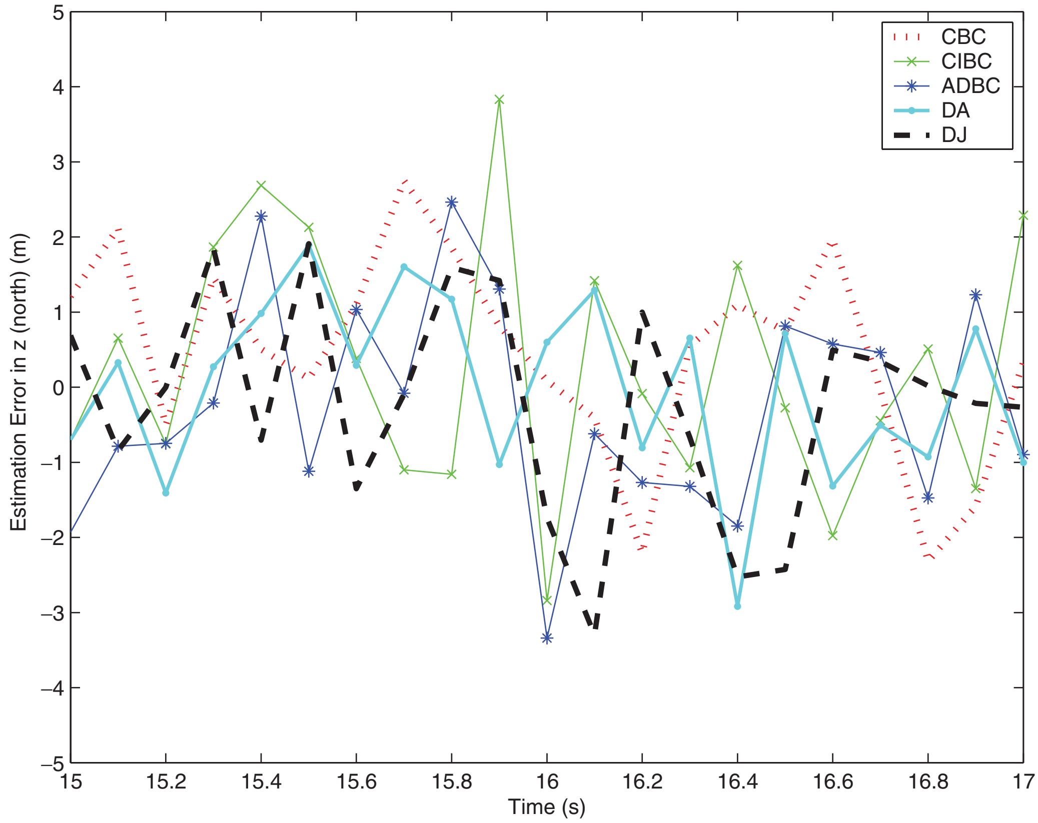


Figure 3. Position estimation error in Z

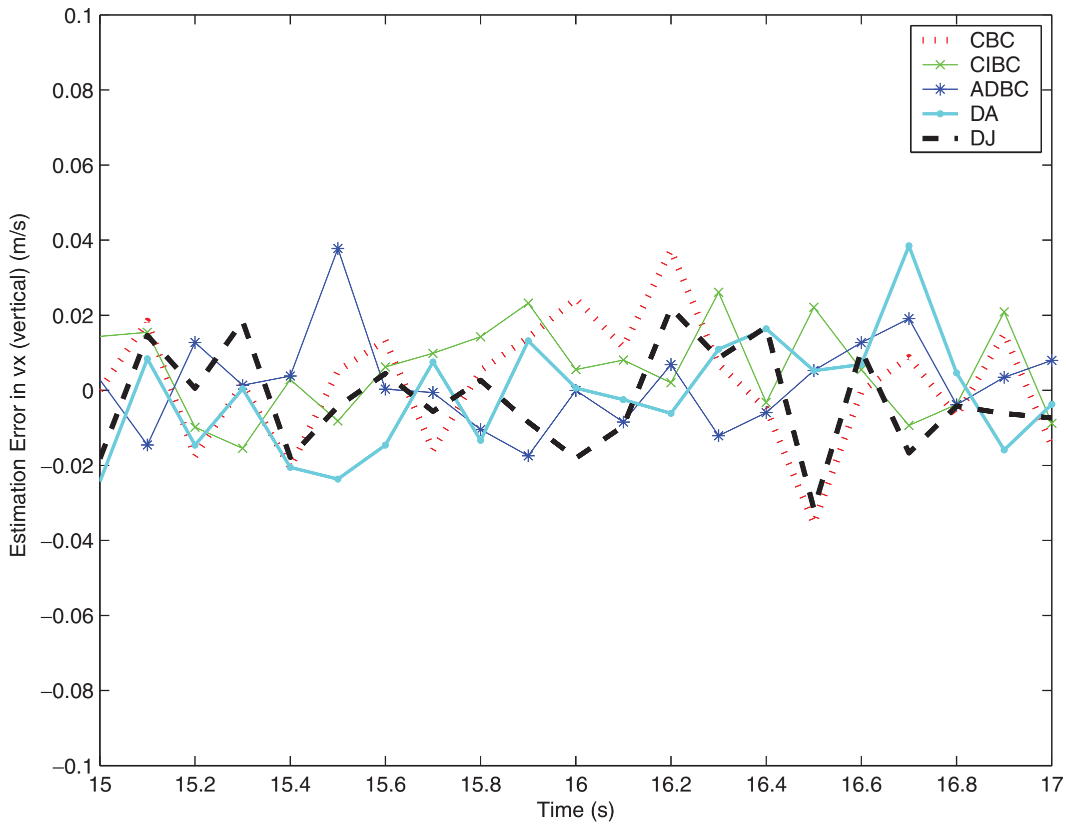


Figure 4. Velocity estimation error in X

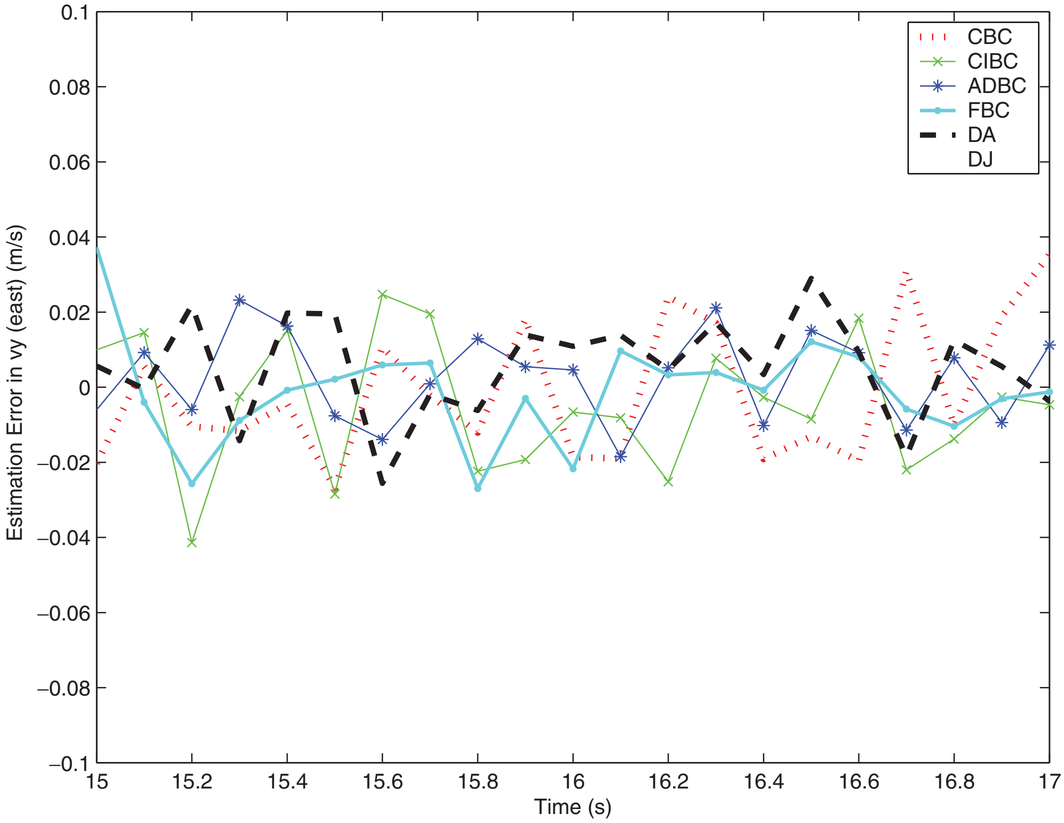


Figure 5. Velocity estimation error in Y

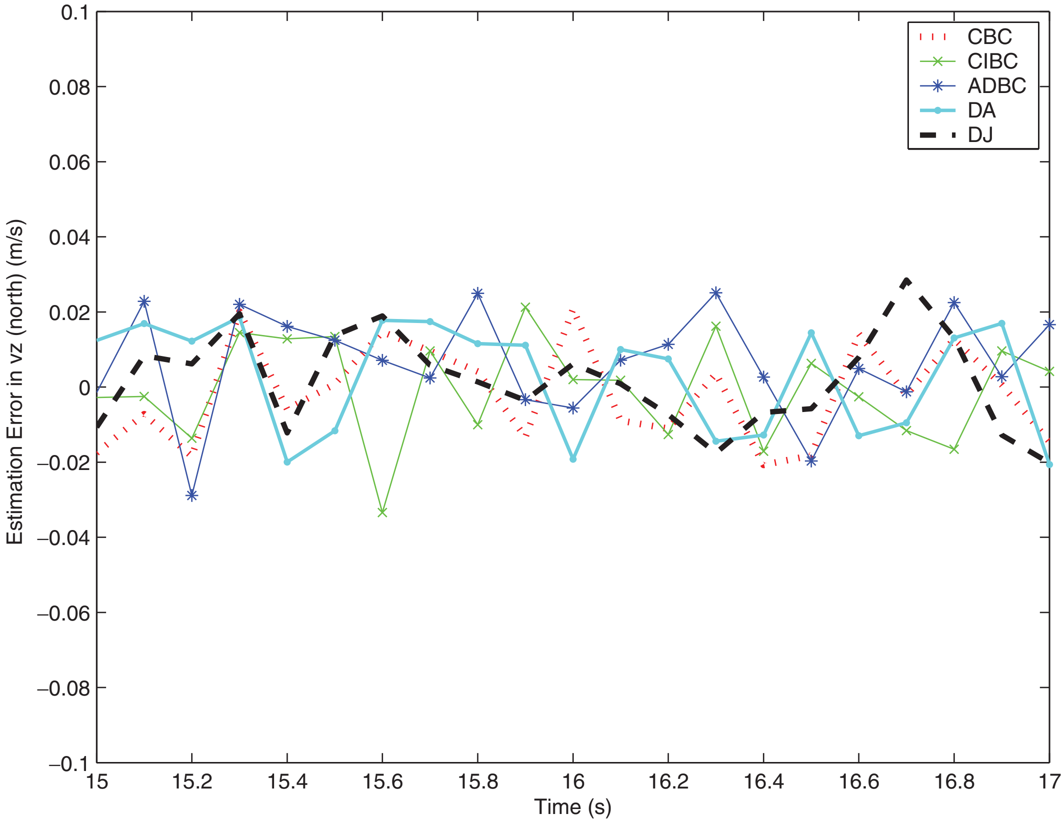


Figure 6. Velocity estimation error in Z

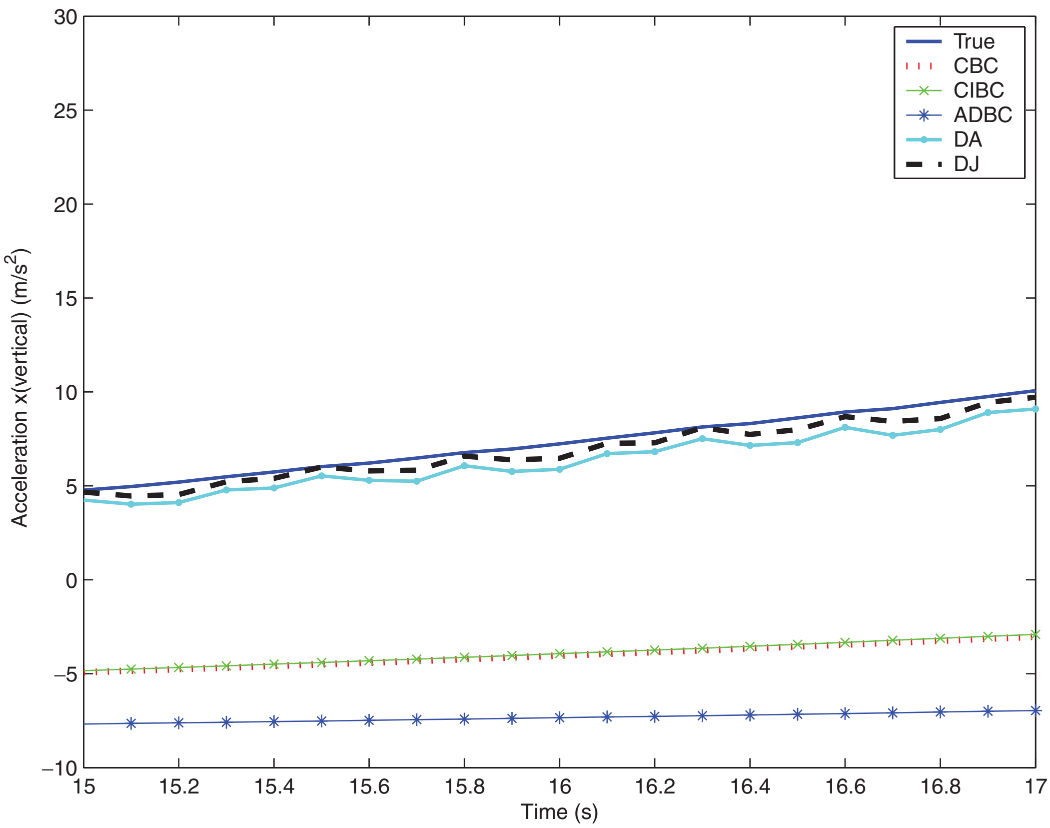


Figure 7. Acceleration estimates in X

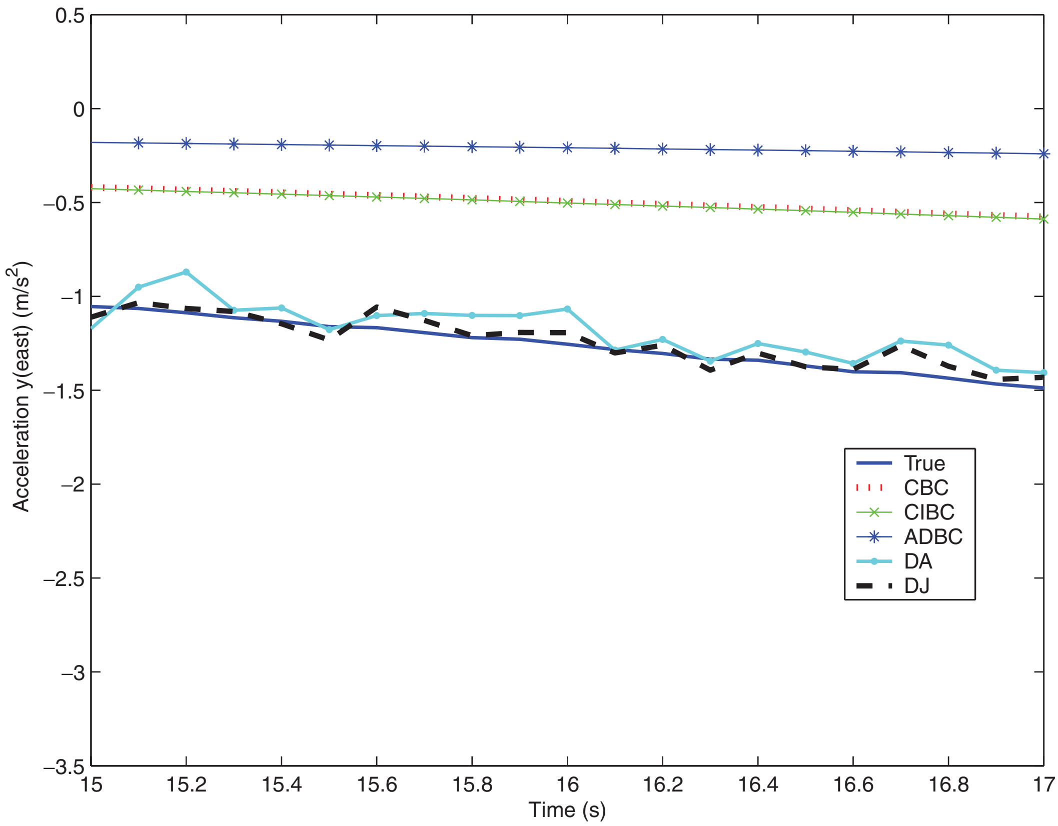


Figure 8. Acceleration estimates in Y

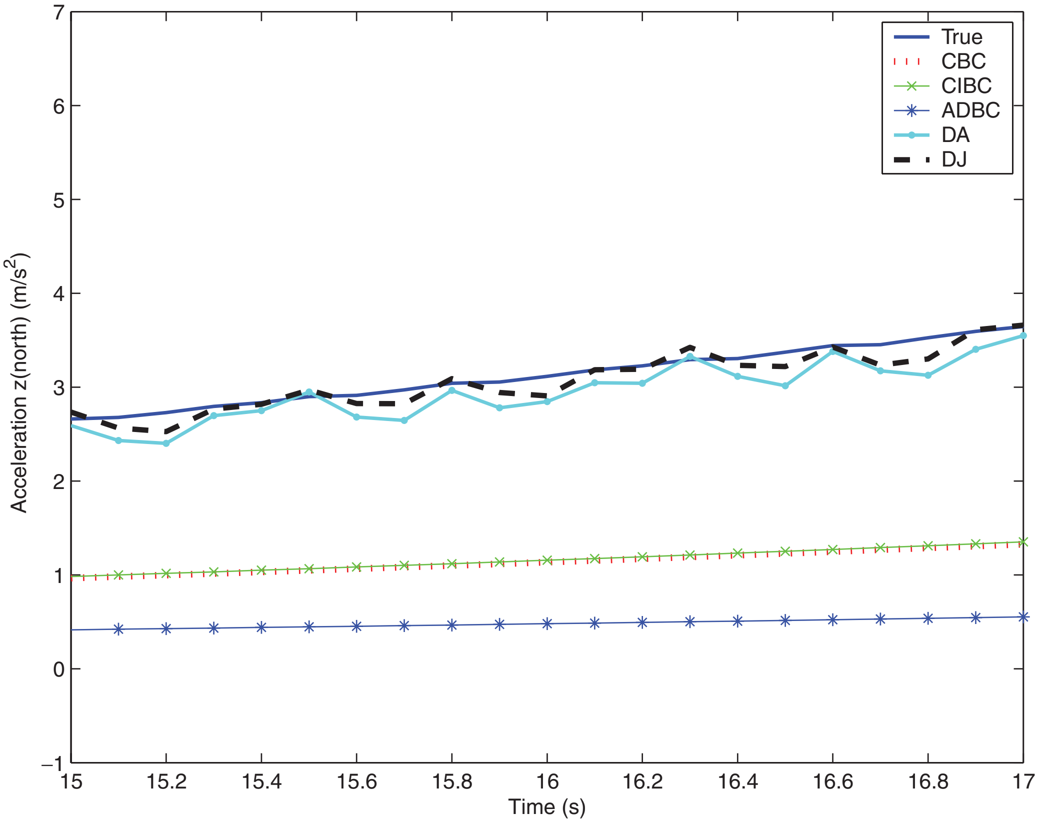


Figure 9. Acceleration estimates in Z